View metadata, citation and similar papers at core.ac.uk
brought to you by CORE
provided by ScholarWorks@UNIST

Resonance properties and microstructure of ultracompliant metallic nanoelectromechanical systems resonators synthesized from Al – 32 at. % Mo amorphous-nanocrystalline metallic composites

C. Ophus, N. Nelson Fitzpatrick, Z. Lee, E. Luber, C. Harrower, K. Westra, U. Dahmen, V. Radmilovic, S. Evoy, and D. Mitlin

Citation: Applied Physics Letters **92**, 123108 (2008); doi: 10.1063/1.2841849
View online: http://dx.doi.org/10.1063/1.2841849
View Table of Contents: http://scitation.aip.org/content/aip/journal/apl/92/12?ver=pdfcov
Published by the AIP Publishing

Articles you may be interested in
Structure and magnetic properties of nanocrystalline Sm 1 s (Fe , Mo) 5 + 2 s
J. Appl. Phys. **105**, 103904 (2009); 10.1063/1.3129566

Noise thermometry and electron thermometry of a sample-on-cantilever system below 1 Kelvin
Appl. Phys. Lett. **92**, 013123 (2008); 10.1063/1.2821828

Design of Q -band loop-gap resonators at frequencies of 34 – 36 GHz for single electron spin spectroscopy in semiconductor nanostructures
Rev. Sci. Instrum. **77**, 064702 (2006); 10.1063/1.2206776

Fabrication and electromechanical properties of a self-actuating Pb (Zr 0.52 Ti 0.48) O 3 microcantilever using a direct patternable sol-gel method
Appl. Phys. Lett. **88**, 042904 (2006); 10.1063/1.2168261

Durability studies of micro/nanoelectromechanical systems materials, coatings and lubricants at high sliding velocities (up to 10 mm s) using a modified atomic force microscope
J. Vac. Sci. Technol. A **23**, 830 (2005); 10.1116/1.1843821

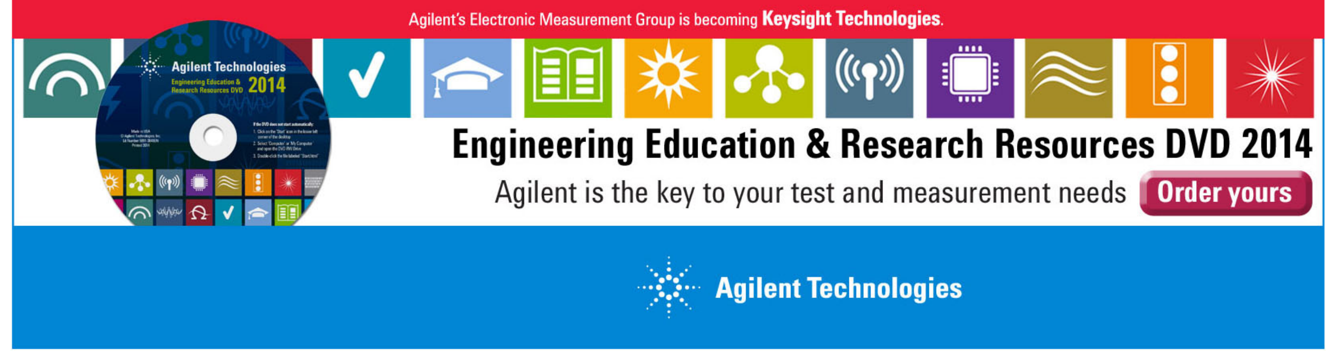

This article is copyrighted as indicated in the article. Reuse of AIP content is subject to the terms at: http://scitation.aip.org/termsconditions. Downloaded to IP: 114.70.7.203 On: Tue, 24 Jun 2014 01:24:16

Resonance properties and microstructure of ultracompliant metallic nanoelectromechanical systems resonators synthesized from Al–32 at. %Mo amorphous-nanocrystalline metallic composites

C. Ophus,[1,2] N. Nelson Fitzpatrick,[2,4] Z. Lee,[3] E. Luber,[1,2] C. Harrower,[1,2] K. Westra,[4] U. Dahmen,[3] V. Radmilovic,[3,a),b)] S. Evoy,[2,4] and D. Mitlin[1,2,a),c)]
[1]*Chemical and Materials Engineering, University of Alberta, Canada T6G-2G6*
[2]*National Institute of Nanotechnology, Edmonton, Canada T6G 2M9*
[3]*NCEM, Lawrence Berkeley National Laboratory, Berkeley CA 94720, USA*
[4]*Electrical and Computer Engineering, University of Alberta, Canada T6G 2V4*

(Received 9 August 2007; accepted 11 December 2007; published online 27 March 2008)

This study details the resonance properties of 20 nm thick nanoelectromechanical system scale cantilevers fabricated from a metallic Al–32 at. %Mo nanocomposite. The advantage of the Al–32 at. %Mo alloy is that its strength and near-atomic surface smoothness enable fabrication of single-anchored metallic cantilevers with extreme length-to-thickness ratios, as high as 400:1. This yields uniquely compliant structures with exquisite force sensitivity. For example, an 8 μm long, 20 nm thick Al–32 at. %Mo device has a spring constant of $K \cong 280\ \mu$N/m. We show through transmission electron microscope analysis and continuum modeling that the relevant damping mechanisms are related to the device microstructure. © *2008 American Institute of Physics*. [DOI: 10.1063/1.2841849]

Two-phase amorphous-nanocrystalline composites may be significantly more ductile than purely amorphous metallic alloys.[1–4] Such microstructures should be well suited for cantilever-based NEMS applications offering a combination of smoothness, strength, and elastic properties. In a previous study,[5] we used room temperature magnetron cosputtering to create Al–Mo films of various compositions. We then tested the films' mechanical and electrical properties, ascertained the surface roughness, and performed some characterization of the microstructure, all as a function of alloy content. The optimum combination of properties was in the Al–32 at. %Mo alloy, which had a two-phase amorphous-nanocrystalline microstructure. The study also reported proof-of-principle fabrication and testing of nanoscale cantilevers and paddles of various geometries. The resonance properties were not, however, treated in any detail. Hence, the goal of this work is to provide a comprehensive treatment of the resonance performance of the 20 nm thick NEMS cantilevers fabricated from the Al–32 at. %Mo alloy films.

Al–32 at. %Mo thin films and single-clamped NEMS cantilever devices were synthesized and characterized in a manner described in Ref. 5. The only variation from Ref. 5 was an improved sputtering base pressure for the film deposition, which in this study is 2×10^{-7} Torr. The tested devices have a thickness of 20 nm, a width of 800 nm, and length ranging from 1 to 8 μm. The cantilevers also possess a 1.2 μm undercut. Resonance testing was performed using a laser-interferometric method described in Ref. 6. The testing was performed at 0.1 Torr and ambient temperature.

Figure 1(a) shows a bank of 20 nm thick Al–32 at. %Mo cantilevers with lengths ranging from 1 to 8 μm. The banks of cantilevers were resonated using the interferometer setup, obtaining the resonance frequencies and quality factors (Q) as a function of device length. Figure 1(b) shows the frequency results of these experiments. The inverse square root of frequency versus length demonstrates a linear relationship, agreeing well with theory,[7]

$$f = 0.1615 \frac{t}{l^2} \sqrt{\frac{E}{\rho}}. \tag{1}$$

Here t is the cantilever thickness, l is the length, and E and ρ are the elastic modulus and density of Al–32 at. %Mo, respectively. The undercut of the cantilevers is roughly equivalent to the x intercept of the best-fit line and is measured as 1.2 μm. This is in good agreement with the undercut measured in scanning electron microscope (SEM) images.

From the slope of the best-fit line, we can extract the average speed of sound $\sqrt{E/\rho}$ in Al–32 at. %Mo as 5369 m/s. Assuming a rule of mixtures, the density ρ of the films is 5130 kg/m^3. This yields a Young's modulus of $E = 147$ GPa for the cantilevers, in agreement with the nanoindentation analysis which gave a value of 120 GPa.[5]

The extreme aspect ratio of these cantilevers makes them very elastically compliant. For a single-clamped cantilever, the spring constant K may be approximated by Eq. (2):[8]

$$K = 0.2427 m \omega^2. \tag{2}$$

The mass of the cantilever is m and ω is the angular frequency ($2\pi f$). Because of their 20 nm thickness, these devices display an unparalleled elastic compliance. For example, the 8 μm long cantilever would have a spring constant of $K \cong 280\ \mu$N/m. Such highly-compliant structures will have major advantages when utilized as supports for AFM/scanning tunnel microscope tips in scanning force microscopy applications, where their electrical conductivity would be also beneficial.

We measured the quality factors for the cantilevers, obtaining a range of quality factor (Q) values from 30 to 245, with an average of 125. Despite the low Q, Al–32 at. %Mo cantilevers can achieve extremely high mass sensitivity due to their low mass and nanoscale thickness. The theoretical mass sensitivity can be approximated as $\Delta m \cong m Q^{-1}$. This

a)Authors to whom correspondence should be addressed.
b)Electronic mail: dmitlin@ulaberta.ca.
c)Electronic mail: VRRadmilovic@lbl.gov.

This article is copyrighted as indicated in the article. Reuse of AIP content is subject to the terms at: http://scitation.aip.org/termsconditions. Downloaded to IP: 114.70.7.203 On: Tue, 24 Jun 2014 01:24:16

 © 2008 American Institute of Physics

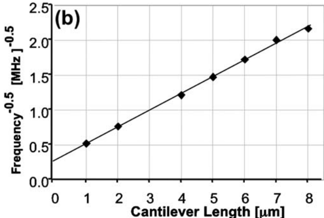

FIG. 1. (A) shows a bank of 20 nm thick Al–32 at. %Mo cantilevers that were resonance tested. (b) shows a plot of the inverse square root frequency vs the cantilever length. The undercut of the cantilevers is roughly equivalent to the x intercept of the best-fit line and is measured as 1.2 μm.

predicts the mass sensitivities of the devices to be in the range of 2×10^{-17} to 3×10^{-19} kg; comparable to that achieved by the most sensitive NEMS resonators.

Figure 2 shows transmission electron microscope (TEM) micrographs of the Al–32 at. %Mo microstructure. Figure 2(a) shows a representative high resolution image. Figure 2(a) shows the microstructure to consist of nanocrystallites densely dispersed throughout an amorphous matrix. Figure 2(b) confirms the presence of a bcc crystalline phase by comparing an experimental and simulated diffraction patterns. The nanocrystallites could be imaged in dark field [Fig. 2(c)] using a portion of the (011) diffraction ring. Significant intensity was also present from the diffuse amorphous diffraction ring. While the exact composition of the two phases could not be identified, analytical TEM did confirm that the crystallites were Mo-rich while the amorphous matrix was Al-rich.

The image in Fig. 2(d) shows the microstructure near the film surface. Because Fig. 2(d) was recorded at higher magnification than Fig. 2(a), the nanocrystallites are more discernable in this image. The dimensions of the nanocrystallites are in the 1–3 nm range. An amorphous oxide layer (arrowed) coats the surface of the film, and is 2–3 nm in thickness. This surface oxide will intrinsically limit the minimum achievable cantilever dimensions at which they are considered metallic. For example, we can now conclude that the thinnest 5 nm Al–32 at. %Mo devices in our previous study[5] were composed largely of an oxide.

Given the unique microstructure and the nanoscale thickness, the fundamental factors limiting the resonance performance of AlMo cantilevers are a key issue. The most widely applied figure of merit for resonators is the quality factor Q, equal to the center frequency divided by the full width at half maximum of the frequency response. The inverse quality factor is equivalent to the energy fraction lost per resonant cycle. The total quality factor Q_T is dominated by the largest source(s) of damping,

$$\frac{1}{Q_T}=\sum_i \frac{1}{Q_i}, \tag{3}$$

where Q_i refers to a specific mechanism of energy dissipation. The mechanisms of energy loss in resonators are (1) clamping losses, (2) thermoelastic dissipation (TED), (3) extrinsic viscous flow damping or molecular damping, (4) squeeze film damping, (5) surface effects, and (6) internal friction.[9–15] We will now analytically consider how energy dissipation mechanisms 1–5 affect Al–32 at. %Mo cantilevers resonated at 0.1 Torr and at ambient temperature. The contribution from internal friction damping cannot be predicted analytically and requires resonance testing at multiple

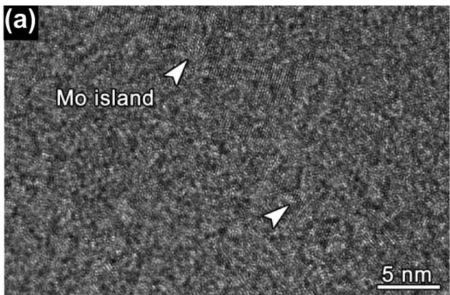

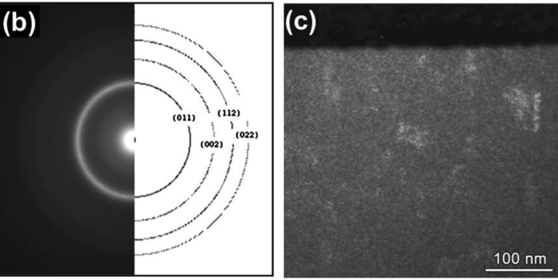

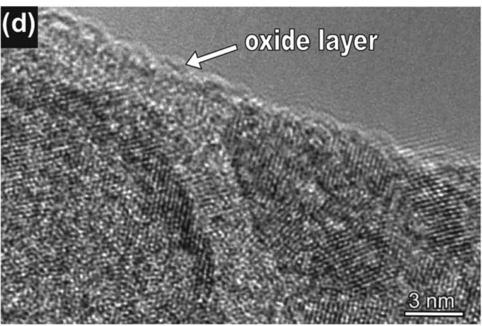

FIG. 2. TEM characterization of the Al–32 at. %Mo film in cross section. (a) shows a representative high resolution image of the microstructure, which consists of nanocrystallites densely dispersed in an amorphous matrix. (b) a comparison of an experimental selected area diffraction pattern with the simulated ring pattern for bcc Mo confirms the presence of a bcc crystalline phase. (c) shows a dark field micrograph of the bcc nanocrystallites imaged using a portion of the (011) diffraction ring. (d) shows the microstructure near the film surface, demonstrating the presence on a surface oxide layer approximately 3 nm in thickness.

temperatures. Its contribution at ambient temperature should be fairly negligible.

If the support is considered to be an infinite elastic sheet, that the clamping losses can be estimated as

$$Q_{\text{clamping}} \approx 0.34\frac{l^3}{t^3}, \tag{4}$$

where l is the cantilever length and t is its thickness.[9] Intuitively, it can be seen that the extremely large length-to-thickness ratio of the AlMo devices makes clamping losses negligible. Due to the 1.2 μm device undercut, the magnitude of the clamping loss could exceed the calculated predictions, but not very significantly.

During resonance, there will be local regions of compression and expansion creating a temperature gradient within the cantilever. This results in irreversible heat flow responsible for TED. The limiting quality factor due to TED is given as

$$Q_{\text{TED}}=\frac{1}{2\Gamma(T)\Omega(T)} \approx \frac{\pi\kappa}{2\alpha^2t^2TEf}, \tag{5}$$

where κ is the thermal conductivity, α is the coefficient of thermal expansion, and T is temperature.[10] The coefficient of

This article is copyrighted as indicated in the article. Reuse of AIP content is subject to the terms at: http://scitation.aip.org/termsconditions. Downloaded to IP: 114.70.7.203 On: Tue, 24 Jun 2014 01:24:16

thermal expansion α and thermal conductivity κ of Al–32 at. %Mo can be reasonably estimated by rule of mixtures of the two elements (Mo: κ=139 W/m K, α=4.8 $\times 10^{-6}$/K; Al: κ=235 W/m K, α=23.1$\times 10^{-6}$/K).

The effects of extrinsic viscous damping can be neglected if the cantilever resonates in the molecular flow regime.[11] If the Knudsen number K_n of a diving board cantilever is greater than 10, it is resonating in the molecular flow regime. The Knudsen number is defined as $K_n = 0.23 k_B T / d^2 P w$, where k_B is the Boltzman constant, d is the average particle diameter of the fluid medium (air, in this case), w is cantilever width, and P and T are pressure and temperature. The resonance properties of the Al–Mo cantilevers were measured in a low vacuum of 0.1 Torr, and assuming $d \sim 0.37$ nm, we find that the Knudsen number of these cantilevers is 640, which is well above the molecular flow lower limit of 10. Therefore, the effects of extrinsic damping can be safely neglected.

In the molecular flow regime, resistive damping due to collision of air molecules with the vibrating cantilever is known as the molecular or Christian damping.[12] The quality factor of molecular damping is

$$Q_{\mathrm{Mol}} = \left(\frac{\pi}{2}\right)^{3/2} \rho t f \sqrt{\frac{RT}{M_m}} \frac{1}{P}, \tag{6}$$

where R is the ideal gas constant, M_m is the molar mass of the gas, and all other quantities are as defined previously.

In the molecular flow regime another potential source of energy dissipation is the film squeeze effect. The losses due this effect are estimated by

$$Q_{\mathrm{Sq}} = (2\pi)^{5/2} \rho t f \left(\frac{d_o}{L}\right) \sqrt{\frac{RT}{M_m}} \frac{1}{P}, \tag{7}$$

where d_o is the distance between the cantilever and substrate.[12] The value d_o was estimated from the SEM images of the cantilevers to be 1 μm.

Due to the extremely high surface to volume ratio of these cantilevers and the oxide layer, it is expected that surface losses will be a large source of energy dissipation. For a wide cantilever with a surface layer of thickness δ,[13] gives the surface losses as

$$Q_{\mathrm{surface}} = \frac{t}{6\delta} \frac{E_1}{E_2^S}, \tag{8}$$

where E_1 is the elastic modulus of the cantilever and E_2^S is the loss modulus of the surface layer. Measurements of the damping ratio and elastic modulus of alumina have been performed by Wolfenden[14] and Fukuhara and Yamauchi,[15] giving an upper bound on the alumina loss modulus of 405 MPa. With a measured thickness of about 3 nm for the surface oxide, this yields a good estimate of surface losses.

Figure 3 plots of the calculated damping contributions in the Al–32 at. %Mo system as a function of device thickness. Equations (3)–(8) were used for the calculation. The device length and width were kept constant at 5 μm and 800 nm. The device thickness was varied two orders of magnitude, from 10 to 1000 nm. A device undercut of 1.2 microns is included in the calculations. The bottom gray line in the plot is the total quality factor. The chart indicates that above 200 nm device thicknesses, "conventional" factors begin to dominate the damping behavior: thermoelastic

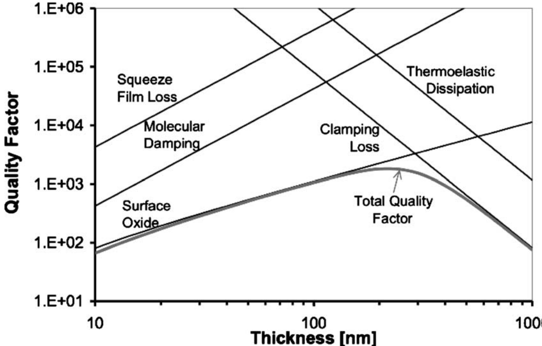

FIG. 3. Damping contributions in 5 μm long, 800 nm wide Al–32 at. %Mo cantilevers as a function of device thickness.

dissipation and clamping losses. At NEMS-scale thicknesses, however, it is the oxide that drives down the device performance. Molecular damping and squeeze film effect would become important if the oxide was not present.

This study serves as a guide on way to increase the detection sensitivity of devices with extreme surface to volume ratios by eliminating surface defects, oxides, or purposely deposited overlayers. For example, a similar microstructure composed of the base element less prone to significant oxidation than Al should offer improved detection sensitivity in parallel with all the advantages of an electrically conductive platform. To this end we have recently developed Au and Ni-based devices[16,17] with improved Q values over Al–Mo.

The authors acknowledge support of the National Center for Electron Microscopy, Lawrence Berkeley Lab, which is supported by the U.S. Department of Energy under Contract No. DE-AC02-05CH11231. This work was also supported by NSERC Discovery Grants, the Alberta Ingenuity Foundation, and by NINT NRC.

[1] C. Fan and A. Inoue, Appl. Phys. Lett. **77**, 46 (2000).
[2] C. C. Hays, C. P. Kim, and W. L. Johnson, Phys. Rev. Lett. **84**, 2901 (2000).
[3] J. Eckert, A. Reger-Leonhard, B. Weiss, and M. Heilmaier, Mater. Sci. Eng., A **301**, 1 (2001).
[4] M. Calin, J. Eckert, and L. Schultz, Scr. Mater. **48**, 653 (2003).
[5] Z. Lee, C. Ophus, L. M. Fischer, N. Nelson-Fitzpatrick, K. L. Westra, S. Evoy, V. Radmilovic, U. Dahmen, and D. Mitlin, Nanotechnology **17**, 3063 (2006).
[6] D. W. Carr and H. G. Craighead, J. Vac. Sci. Technol. B **15**, 2760 (1997).
[7] P. G. Datskos, T. Thundat, and N. V. Lavrik, *Encyclopedia of Nanoscience and Nanotechnology* (American Scientific, Stevenson Ranch, CA, 2004), Vol. 10, p. 1.
[8] J. E. Sader, J. W. M. Chon, and P. Mulvaney, Rev. Sci. Instrum. **70**, 3967 (1999).
[9] H. Hosaka, K. Itao, and S. Kuroda, Sens. Actuators, A **A449**, 87 (1995).
[10] T. V. Roszhart, Proceedings of the Solid State Sensor Actuator Workshop, 1990, p. 13.
[11] R. B. Bhiladvala and Z. J. Wang, Phys. Rev. E **69**, 036307 (2004).
[12] M. H. Bao, H. Yang, H. Yin, and Y. Sun, J. Micromech. Microeng. **12**, 341 (2002).
[13] J. L. Yang, T. Ono, and M. Esachi, J. Microelectromech. Syst. **11**, 775 (2002).
[14] A. Wolfenden, J. Mater. Sci. **32**, 2275 (1997).
[15] M. Fukuhara and I. Yamauchi, J. Mater. Sci. **28**, 4681 (1993).
[16] N. Nelson-Fitzpatrick, C. Ophus, E. Luber, L. Gervais, Z. Lee, V. Radmilovic, U. Dahmen, D. Mitlin, and S. Evoy, Nanotechnology **18**, 355303 (2007).
[17] E. Luber, R. Mohammadi, C. Ophus, Z. Lee, N. Nelson-Fitzpatrick, K. Westra, S. Evoy, U. Dahmen, V. Radmilovic, and D. Mitlin, Nanotechnology **19**, 125705 (2008).

This article is copyrighted as indicated in the article. Reuse of AIP content is subject to the terms at: http://scitation.aip.org/termsconditions. Downloaded to IP: 114.70.7.203 On: Tue, 24 Jun 2014 01:24:16